1
Introduction

1.1 Nanomaterials

Nanomaterials refer to materials that have characteristic features in the range of 10^{-9} m. The nanomaterial with size, shape, and properties offers a wide range of advantages over the bulk counterpart. Nanomaterials can be tailored for various applications, and their versatility in tuning the properties has gained the attention of researchers from the past decade. The change in the properties at the nanoscale is due to the quantum confinement effect.[Cai et al., 2017] The optical properties, electrical properties, mechanical properties, magnetic properties, etc., are also a function of particle size and geometry.[Kolahalam et al., 2019] This effect is not seen in the macroscopic to micrometer dimensions of the materials, but it becomes more significant in the nano range. The biggest advantage is their high surface area, which increases their demand for a wide variety of industrial applications (Figure 1.1). [Khin et al., 2012]

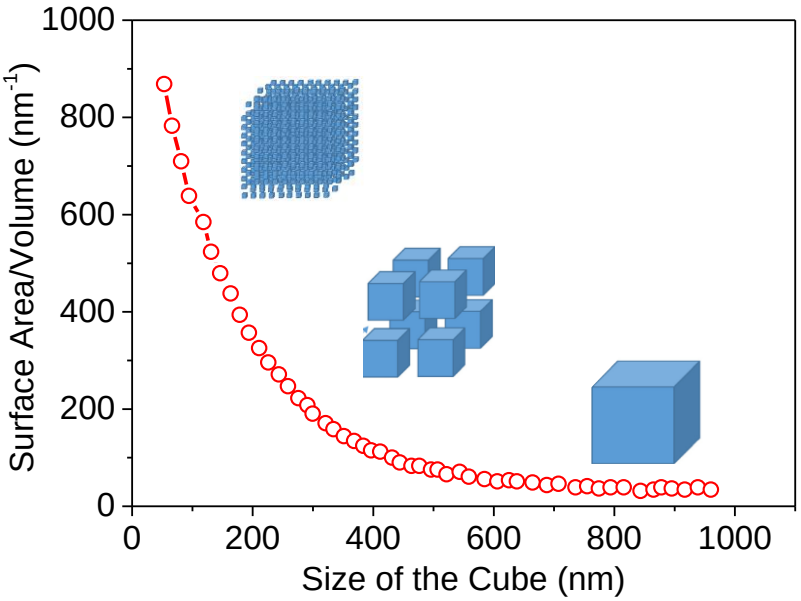

Figure 1.1: Schematic representing the increased surface area to the same volume of a cube. Figure adapted from reference [Paladiya et al., 2018]

1.2 Nanomaterials for Energy Applications

As the global population, the energy demand is also increasing, leading to the search for alternative energy production methods and energy storage. Energy is one of the significant cornerstone keys that play an essential role in the overall sustainable development of society and its economy. Sustainable energy production is one of the major challenges faced by research around the world. [Tahir et al., 2017] The limited reserves of fossil fuel, increasing demand, and increasing cost of this fuel have led to the search of different energy production and storage. Nanomaterials play an important role in enhancing the properties of the materials, as discussed in the section above. The nanomaterials have been widely used in various energy storage, production, and generation such as solar cells, fuel cells, supercapacitors, batteries, thermoelectrics. This section of the thesis is focused on the Oxygen Evolution Reaction (OER) and Supercapacitors as energy applications.

Multiple materials have been explored for water electrolysis for hydrogen evolution reaction (HER) and oxygen evolution reaction (OER).[Gong et al., 2015] Due to the advantages of the wide availability of water resources, the high purity of hydrogen, and the feasibility of large-scale production, electrochemical water splitting provides a promising method to produce hydrogen via OER.[Busupalli et al., 2016; Hisatomi et al., 2014; Mondschein et al., 2017; Tee et al., 2017] IrO_2 and RuO_2 catalysts are known to deliver excellent catalytic performance in OER.[Babar et al., 2018; Subbaraman et al., 2012; Zhu et al., 2017c]

1.2.1 Importance of OER and Mechanism

Electrolysis of water is the best method to produce ultra-pure hydrogen on a large scale with a short time span and reduced environmental pollution. This attractive option can be made viable by improving the OER performance. The basic electrochemistry involved in water electrolysis is expressed below. The electrochemical splitting of water into hydrogen and oxygen gas at neutral pH conditions can be given as follows:

$$H_2O\,(l) \rightarrow H_2\,(g) + 1/2O_2\,(l) \ldots\ldots\ldots\ldots @E_0 = 1.23\ V\ vs.\ RHE \qquad (1)$$

As seen from the above equation, it needs standard 1.23 V vs. RHE of potential for water splitting. However, accompanying it, there are various resistance and energy losses, which leads to overpotential. The overpotential during the water electrolysis can be reduced by using highly acidic conditions or in highly alkaline conditions. The schematic of water electrolysis in the alkaline medium is as shown in Figure 1.2a. There are certain advantages and disadvantages when the electrodes are subjected to these extreme pH conditions.
The use of noble metals can enhance efficiency but at the cost of the high price of the noble metals. In this context, OER catalyzed by 3d transition metals and their oxides/hydroxides is one of the best choices of materials as they are stable and can work efficiently in alkaline conditions. Still, the challenge of overpotential prevails because of the poor hydrogen evolution, as the alkaline electrolyte cannot supply protons instantly and constantly for water splitting at high pH. The following reactions can be proposed that can occur in acidic and alkaline electrolytes with water splitting.

In acidic medium (1 M H_2SO_4)

$$2H_2O\,(l) \rightarrow 4H^+\,(aq) + 4e^- + O_2\,(g)\ (at\ anode) \qquad (2)$$
$$4e^- + 4H^+\,(aq) \rightarrow 2H_2\,(g)\ (at\ cathode) \qquad (3)$$

In basic medium (1 M KOH)

$$4OH^-\,(aq) \rightarrow 2H_2O\,(l) + 4e^- + 2O_2\,(g)\ (at\ anode) \qquad (4)$$
$$4e^- + 4H_2O\,(l) \rightarrow 4OH^-\,(aq) + 2H_2\,(g)\ (at\ cathode) \qquad (5)$$

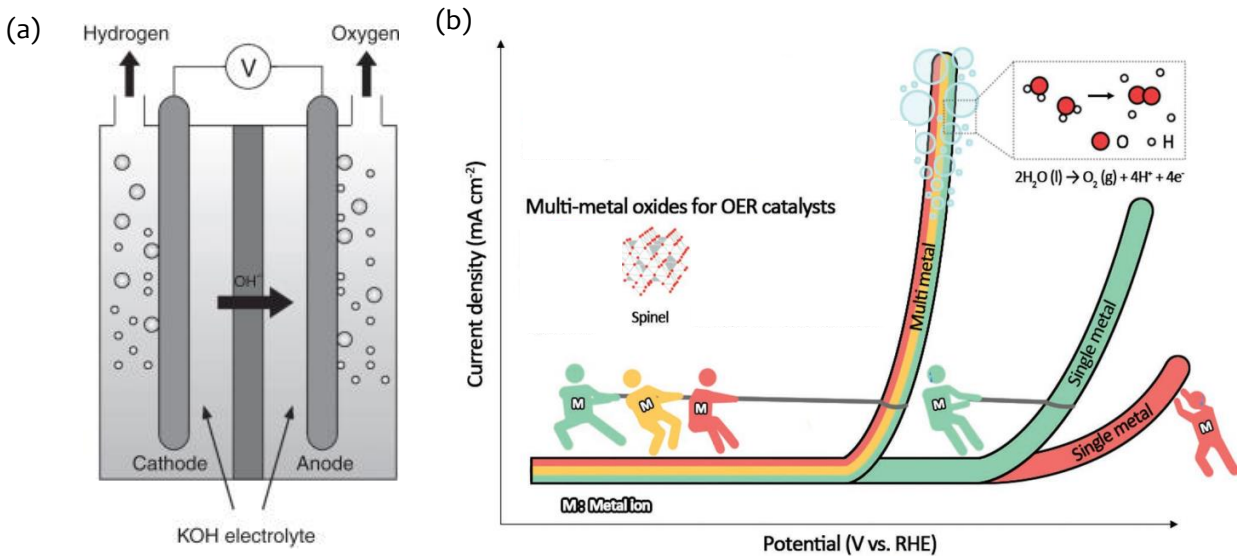

Figure 1.2: (a) Schematic showing Oxygen Evolution Reaction (OER) in KOH electrolyte (b) Importance of oxides for OER. Figures adapted from reference (a) [Greig et al., 2017] and, (b) [Kim et al., 2018b].

1.2.2 Ni-Co Oxides as Electrocatalyst for OER

Nanomaterials, as discussed above, provide phenomenal mechanical, electrical, and magnetic properties with a high surface area for hydrogen production. Nanomaterials based on noble metals have been widely explored in the literature, but nanomaterials based on non-noble materials are being explored due to the limited resources. The transition metal oxides have gained attention recently as catalysts for OER due to their several advantages. The Ni and Co oxides are studied well in the literature for OER. These metal oxides are comparatively cheaper and easier to obtain than the noble metal oxides making them more feasible for commercial applications. In addition to the cheap cost transition metal, oxides can be easily tuned for the desired composition with other elements introducing the possibility of synergistic effect, which can combine to give good OER performance. The transition metals can form more than one cationic oxidation state, helpful in adding the oxidation and reduction that occurs within an electrolytic cell (Figure 1.2b). The cationic species can quickly shift the oxidation states, which in turn improves stability. The crystal structure of electrocatalysts has a considerable influence on catalytic activity performance. They have an affinity for oxygen adsorption but are not strong enough that they buildup on the catalyst. The efficiency of an electrocatalyst can be tuned by the introduction of vacancies in a lattice structure to some extent. Apart from the above parameters, the electrocatalyst should also have a considerable high surface area to facilitate the active catalytic sites for the reaction.

The transition metal oxides are present in various ordered structures and are available in amorphous structures, which can be manipulated to optimize the OER performance. For e.g., NiO with different phases were synthesized by direct current sputtering with Ni target at 500 °C in an unbalanced magnetron cathode with MgO substrates. The least overpotential of 320 mV was observed in 110 oriented NiO with a Tafel slope of 40 mV. [Poulain et al., 2018] Ultrasmall Ni/NiO nanoclusters on thiol-functionalized exfoliated GO nanosheets were synthesized using a multistep sonication process. The synthesized material shows a Tafel slope of 46 mV/dec and an overpotential of 270 mV.[Munir et al., 2019] N doped NiO sheets were synthesized using a hydrothermal process, and the material showed an overpotential of 270 mV.[Qian et al., 2019] The most commonly occurring structure in the category of transition metal oxides is the spinel structure. The spinels contain more than one type of cation, which has the versatile ability to switch the positions of the cations, which can enhance the overall activity of the catalyst. Multiple cations of the same element may prove helpful in the transfer of electrons that occurs during both the OER and the Oxygen Reduction Reaction (ORR). The

transition metal oxides show some degree of electrical conductivity but are lower than desired than what is desired for electrocatalyst. The spinel structure of many transition metal oxides due to their vacancies and lattice defects helps increase the material's conductivity. The Co_3O_4 spinel is also studied largely in literature. The Co_3O_4 synthesized by the hydrothermal method with varying Co^{3+} content exhibited an overpotential of 380 mV. [Alex et al., 2020] Co_3O_4 electrocatalytic film prepared by a chemical solution deposition method. showed a low overpotential of 377 mV. [Jeon et al., 2015]

The large-scale fabrication of nanomaterials without binders and additives with ease is the burning topic. The poisoning of electrodes during OER is triggered in various ways like catalyst leaching, structural reconstruction, and irregular aggregation of the active material on the electrode surface. Another non-negligible stability problem is the peeling of catalyst material from substrates during OER at moderate current densities for long durations when additives and binders are used. They also degrade the OER performance due to increased internal resistances that increase the overpotential. Therefore, developing highly active oxygen evolution electrodes that can possess a significantly prolonged catalytic lifetime (e.g., beyond thousands of hours) remains a significant challenge.[Liu et al., 2018e] Hence, alkaline water electrolysis has been an exciting topic for studies and is one of the main objectives of this thesis.

1.2.3 Importance of Supercapacitors

The energy produced using various techniques in the form of electricity needs to be stored for which batteries, supercapacitors, and various energy storage devices are being explored. Supercapacitors have gained tremendous attention because of their outstanding features, including high power density, quick charging and discharging rates, low maintenance, excellent stability, long cycle life, and safe operation, making them a next-generation system for potential applications in energy storage devices. Recently, supercapacitors have gained popularity in emergency doors in flights. The supercapacitors available in the market have a power density of less than 10 Wh/kg, which is lower than batteries and fuel cells and cannot be used in portable devices and electric vehicles for energy storage.

1.2.4 Working Principle of Supercapacitors

As with traditional capacitors, Electric Double Layer Capacitors (EDLCs) store energy by a similar principle of charge separation (Figure 1.3).[Simon et al., 2014] The main difference between EDLCs and traditional supercapacitors is the capacitance value. In EDLCs, the higher capacitance values are achieved through the high surface area of porous materials (usually, these are carbon materials) compared to the conventional capacitor plates.[Simon et al., 2008] EDLCs can store substantially more charge than a traditional capacitor in several orders of magnitude because of the following reasons:

1) The increased high surface area is because of the extended porous structure of the electrodes.
2) The small thickness of the electric double layer formed at electrode-electrolyte interphase.

Similar to lithium-ion batteries, EDLCs are charge storage devices. EDLC comprises two electrodes, a separator, and an electrolyte. The function of a separator is to electrically insulate the electrodes in the assembly. As shown schematically in Figure 1.3, the separation of electric charges results in the electrical double-layer capacitance because of the directional alignment of ions and electrons at the electrode-electrolyte interface. The electric charges are collected on the electrode surface, while electrolyte ions with opposite charges accumulate in the solution to maintain electrical balance. If the system is subjected to the external load, the ions in the electrolyte travel towards the oppositely charged electrode and vice versa to complete the circuit. When the load is lifted off, the charge migration takes place in the opposite direction leading to the discharge. During the charge-discharge process, the concentration of electrolyte

does not change regardless of the process. In the charging and discharging process of the EDLC, the electrode material does not react electrochemically, and there is only physical charge accumulation at the solid/electrolyte interface.

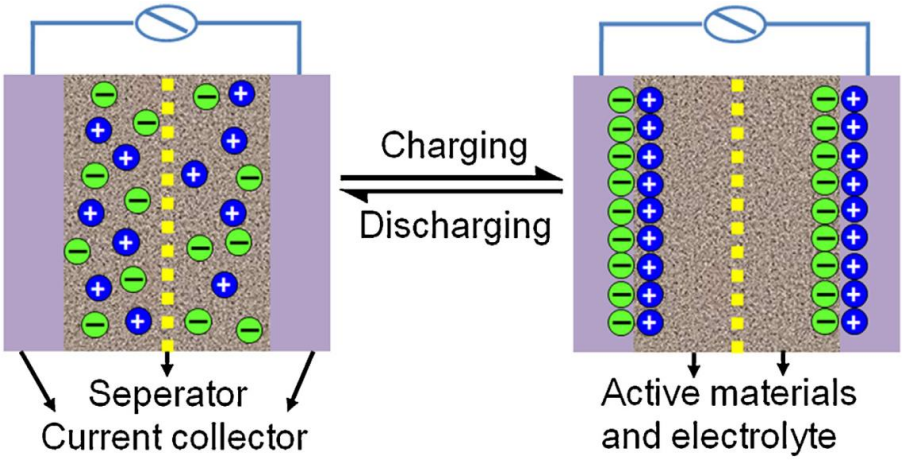

Figure 1.3: A schematic of charging and discharging of an EDLC supercapacitor. Adapted from reference [Chen et al., 2013b].

The single electrode and electrolyte interface makes a single capacitor, and the complete unit is a set of two separate capacitors that are connected in series in the form of electrodes. EDLCs have a high capability of charge-discharge and remain stable at specific temperatures for longer durations. The binders and additives, active materials (catalysts), intercalation, temperature, porosity, surface area, and capacitance also affect the electric double-layer capacitance. The performance of EDLCs supercapacitors is highly dependent on the physical and chemical characteristics of the electrodes.

1.2.5 Synthesis Methods of Carbon-based Electrodes for Application as Supercapacitors

In recent years, comprehensive research has been actively dedicated to increasing the gravimetric energy density and lowering the fabrication costs of supercapacitors without sacrificing their high power delivery and cycle life. In literature, efforts have been made for the fabrication of carbon-based electrodes with Ni-based compounds that can be carried out as a composite for additional enhancing the supercapacitor performance. For e.g., carbon/$Ni(OH)_2$ composite was prepared by various treatments on rice husk. The supercapacitor showed a high ~952 F/g at a current density of 1.0 A/g with 81.3% capacitance retention for 1000 cycles.[Cai et al., 2020] Activated graphene-based carbon electrodes with $Ni(OH)_2$ from rice husk were prepared with a two-step chemical process, and synthesized carbon had 3292 m^2/g specific surface area. The fabricated electrodes had a specific capacitance of 300 F/g at a current density of 50 mA/g.[Yeleuov et al., 2020] Nitrogen and phosphorous doped carbon cloth with bimetallic Ni and Co hybrid electrode delivered a high specific capacitance of 2660 F/g at a current density of 2 A/g and 88.6% capacity retention after 15000 cycles.[Hua et al., 2019] All these fabricated electrodes need sophisticated techniques for fabrication; moreover, they need additional binders and additives that may hinder the supercapacitor performance. Supercapacitors are expected with higher stability, durability, and performance. The surface area plays a vital role in the charging and discharging process; hence, carbon nanomaterials can fulfill all the above parameters with a higher surface area. The synthesis of carbon has been carried out using chemical vapor deposition (CVD), ion beam sputtering, ionized deposition method, pyrolysis of polymer and hydrocarbon, plasma synthesis, and hydrolysis wood, laser ablation, and arc discharge, etc. in the literature as discussed above.

The most effective and promising strategy is to synthesize nanostructured materials with optimized design for high performance. To be more specific, the electrochemical properties can be highly improved through various design strategies such as

1. Incorporation of pseudocapacitive materials like metal oxides, electrically conducting polymers into various grades of conductive carbon materials
2. By increasing the specific surface area (SSA) with pore sizes and pore size distribution of the electrode materials without sacrificing the electrical conductivity.
3. Synthesis of nanosized redox materials with large surface areas to provide sufficient catalytically active sites.
4. To ensure the number of electrolyte ions and electrons participating in the redox reaction, doping the heteroatoms into nanomaterials, making a composite.[Yuan et al., 2020]

In this thesis work, we have focused on the usage of solution-processed Ni-based catalyst for conversion of waste polystyrene to graphitic carbon for energy application as EDL Supercapacitor.

1.3 Nanomaterials for Biosensing Applications

1.3.1 Importance of Glucose Sensor

Healthcare has gained much attention because of the diseases such as diabetes, gout, etc. The people are looking forward to a healthy lifestyle, where awareness of biomarkers is needed to the people from day to day basis; hence, the market demands should have point-of-care healthcare devices necessary to monitor biomolecules/parameters detection. The biosensors are used for point-of-care devices and can also be used for qualitative testing in industrial applications.[Lv et al., 2018] As seen in the previous sections, nanomaterials are widely preferred because of their tunable properties. Nanomaterials have increased the performances and enhanced sensitivities with a lower limit of detections (LODs) in the nanomolar range of concentrations.[Dhara et al., 2019] The significant advantage of nanomaterials is the high surface area offered by the nanostructured nanomaterials. One of the commonly employed techniques is the immobilization of bioreceptor molecules units onto the nanomaterial for electrochemical sensing. The electrochemical sensors assure the reproducibility of the device compared to the other technique. In this context, diabetes is a prevalent dreadful disease. The majority of people around the world are suffering from various issues because of high blood sugar. For the prevention of high blood glucose, it is necessary to monitor it regularly. The most commonly preferred method is through glucose sensors. The commonly available sensors in the market are enzymatic glucose sensors; however, there is a dire need to develop low-cost, disposable, and stable non-enzymatic glucose sensors.

1.3.2 Working Principle of Non-Enzymatic Glucose Sensing

The word enzymatic glucose sensor itself means it contains enzymes. The glucose sensor commonly available in the market uses the enzyme glucose oxidase to catalyze glucose. The glucose oxidase enzyme acts as a catalyst for glucose oxidation to convert them into gluconolactone and hydrogen peroxide. The hydrogen peroxide generated at the electrode is detected and related to glucose concentration in the blood sample. The enzyme-based sensors have limitations because of their high cost, low reproducibility, and poor stability. The enzymatic activity of sensor strips is mainly affected by humidity, temperature, pH, and chemicals. Thus, a non-enzymatic sensor is a suitable alternative to address the challenges discussed above. The nanostructured materials offer enzyme-like activity and act as electrocatalysts to oxidize glucose. This oxidation of glucose generates an electrical current, which is sensed by the electronic circuits. The non-enzymatic sensors offer several advantages like longer storage life, high selectivity/sensitivity, and a simple modification process. Two theories have been widely used for explaining the glucose-sensing mechanism, as shown in Figure 1.4a. D Pletcher proposed the very first model based on chemisorption for non-

enzymatic glucose sensing. According to the theory, as soon as the adsorption process of glucose starts, the molecules start oxidizing due to unfilled d-orbitals of the transition metal atoms, resulting in the bond formation with the adsorbates. It is observed that the hydrogen removal takes place simultaneously with the adsorption of the species on the electrode surface, as shown in Figure 1.4a. The removal of the hydrogen atom during this process is the rate-determining step in most non-enzymatic glucose sensing. Hence, the increased surface area can contribute to faster kinetics leading to enhanced glucose oxidation. The chemisorption model only explains the adsorption process but fails to consider the oxidative role of hydroxyl radicals in the electrolyte solution. Another theory was proposed by L. D. Bruke, known as the ''incipient hydrous oxide adatom mediator'' (IHOAM) model. The model proposed by Bruke was based on the observation that "active metal atoms on the surface underwent a pre-monolayer oxidation step that formed a thin hydrous oxide layer of reactive OHads." This model was based on the observation that "surface-active metal atoms went through an oxidation step before the monolayer, which formed an incipient hydrated oxide layer of reactive OHads. As seen from Figure 1.4b, the proposed process shows both oxidative and reductive processes are catalyzed on the metal surface. As seen from both theories, it can be concluded that nanomaterials with high surface area, good ionic and electrical conductivity, structural modifications, and high electrocatalytic activity are highly essential for enhancing the performance of non-enzymatic glucose sensors.

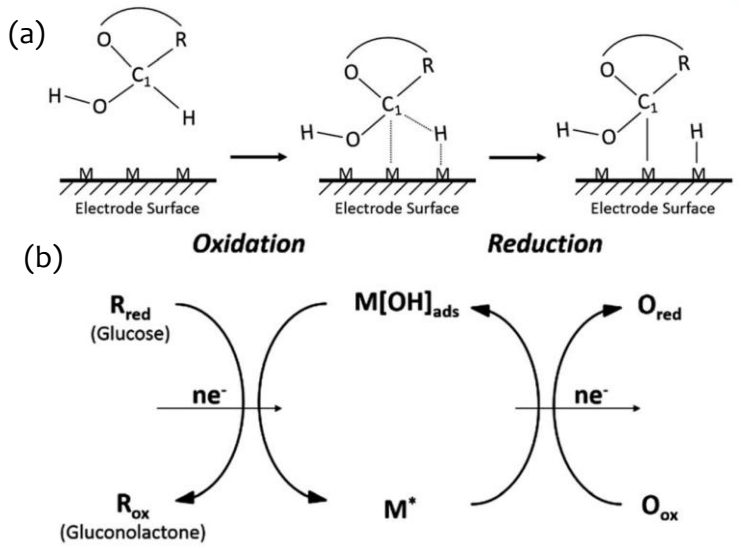

Figure 1.4: (a) Scheme of the activated chemisorption model (b) Scheme of the incipient hydrous oxide adatom mediator model. Figure adapted from reference [Zhu et al., 2016].
Note: M: metal atom on the electrode surface; C1: carbon atom; R: other components of the glucose molecule, M[OH]ads is the oxidative adsorbed hydroxide radical, and M* is the reductive metal adsorption site.

1.3.3 Nickel Oxide-based Non-enzymatic Glucose Sensing

Ni as a transition metal has great potential as an electrode material for sensors because of its natural abundance, low toxicity, low cost, and excellent electrochemical property with stability in an alkaline medium. A variety of NiO nanostructures like hollow spheres and cages, core-shell structures have been explored for application in non-enzymatic glucose sensing. Ni-based $Ni_{60}Nb_{40}$ nanoglass was prepared by using magnetron sputtering followed by compaction at 1.4 GPa under vacuum. The fabricated electrode showed the best performance in terms of sensitivity (20 mA/mM cm^2) and a limit of detection of 100 nM. The excellent performance and enhanced sensitivity towards glucose-sensing were attributed to the extensive network of glassy interfaces.[Bag et al., 2020] Ni-Sn sulfide nanocomposite was synthesized using microwave treatment for 15 min at a constrained temperature of 100 ^oC. The biosensor was fabricated using Ni foam, which shows an excellent sensitivity of 1622.9 μA/mM cm^2 with a

LOD of 0.18 µM. The high activity towards glucose oxidation is because of the improved surface area, stable morphology, more active sites, and surface-controlled redox property. [Chandrasekaran et al., 2021] Ni-Co nanoneedles were synthesized over Fluorine-doped Tin oxide (FTO) and carbon cloth (CC) substrates using a hydrothermal process. The fabricated electrodes show a very high sensitivity of 3 mA/mM cm^2 because of the exposed surface area.[Pathak et al., 2021] Nickel cobalt layered double hydroxide and cobalt copper carbonate hydroxide hierarchical nanostructure on Cu foam was synthesized using a hydrothermal method and then was embedded with a custom-printed circuit board (PCB). The fabricated chip-based sensor demonstrated the feasibility of glucose detection with a linear range of 15–335 µM and a sensitivity of 10.28 µA/µM cm^2.[Pathak et al., 2021] Worm-like Ni_3S_2 nanowires were electrodeposited on the PEDOT-rGO surface of a glassy carbon electrode through cyclic voltammetry. The electrodeposited sensor exhibits a sensitivity of 2123 µA/ mM cm^2 with a wide linear range of 15-9105 µM and 0.48 µM lower detection of limit.[Meng et al., 2021] All these methods discussed used hydrothermal, electrodeposition, sol-gel, and microwave, etc. These techniques suffer from a significant problem of large-scale fabrication and need binder/additives for the active material, reducing the performance. While synthesis of active electrode material and fabrication of electrodes is one of the major tasks, another remains the transparency. Since optically transmitting yet conducting electrodes in biosensors is gaining popularity, they can be used in daily lives, such as contact lenses and display devices.[Elsherif et al., 2018] Moreover, simultaneous detection by electrochemical and optical methods requires the development of functional yet transparent electrodes. Indium-doped Tin Oxide (ITO) and (FTO) have been used to manufacture transparent optical biosensors as these are conductors and transparent in the visible region.[Bobrowski et al., 2018] However, ITO and FTO thin film have limited surface area due to planar geometry that limits either the transparency or the ultimate performance of the device. Thus, disruptive technology is necessary based on the fabrication and transparency for the above-discussed points. In this thesis, we have tried to address the problem of large-scale fabrication and transparency together.

1.3.4 Ni-Co oxide-based Non-enzymatic and Simultaneous Biomolecular Detection

As seen in the case of glucose, the balance of Uric Acid (UA) and Dopamine (DA) in the human body are essential for physiological functions. These biomolecules are present in many biological matrices and are thus essential biomolecules in human physiological processes. AA plays an essential role in tissue repairing. DA is a neurotransmitter in the central nervous systems responsible for renal, hormonal control, and other central nervous system-related activities. UA is a vital biomolecule, and its higher amounts in body fluids can be associated with gout, hyperuricemia, and Lesch–Nyhan syndrome. Therefore, it is essential to develop a biosensor to simultaneously detect the three biomolecules with accurate concentration to diagnose the imbalance in these biomarkers. The electrochemical technique is the most commonly employed technique for the quantitative detection of DA and UA biomolecules. Nevertheless, the simultaneous detection of these biomolecules in the same mixture solution has been challenging because of the close oxidation potentials of DA and UA. Thus, it is technically difficult for simultaneous detection of all three biomolecules complex with bare electrodes. The recent development in sensing material synthesis has shown the possibility of detecting these four molecules simultaneously with chemically modified electrodes. In this thesis work, the electrocatalytic property of Ni-Co oxide has been explored for the biosensing of uric acid and dopamine as necessary biomarkers related to health conditions.

1.4 Nanostructured Electrode Fabrication using Functional Inks

As discussed in the above sections, with the recent advances in the energy and healthcare sector, the development of high-performance devices in compact form is desirable. The fabricated devices necessarily need three aspects for sustaining as a product in the market.

1. Industrially scalable synthesis of electrocatalytic nanomaterials
2. Rational design of electrodes
3. High-resolution patterned devices

Modern technology demands devices to be stretchable and flexible for various applications pertaining to their compressed structure, twist ability, and conformability to 3D non-planar substrates. Hence, there is an immense need to develop sustainable manufacturing technology, which can easily fabricate devices on-demand at a reasonable cost. [Shi et al., 2019] The 3D substrates can effectively increase the performance, activity, and stability when the nanomaterial is uniformly coated. [Parvanian et al., 2020] [Ikram et al., 2020] The majority of the techniques fail to achieve this task. Additionally, materials synthesized using other techniques like hydrothermal, arc discharge, templated method, sol-gel, etc., need binders and additives for coating onto the substrates. In this context, the solution-processable method is the best choice since the desired material can be coated on the substrate with ease and in a controlled way.[Lee et al., 2019]

The Ni-Co-based functional inks offer a promising future for scalable production of these wearable and portable devices. As compared to the other conventional techniques, the use of these functional inks as electrocatalysts using printing/patterning technologies can enable easy customization, rapid and scalable production, and a reduction in material waste. The advent of solution-processed methods with functional inks has attracted much interest from the scientific community. The use of these inks offers promise economic and large-scale fabrications of devices for advances in technological applications. The solution-processable functional inks can offer significant merit over existing methods to manufacture electrochemical devices for energy and biosensing applications. These advantages can be listed as

(1) The ease of controlling thickness.
(2) Tunable ink composition and physical properties.
(3) Reduced fabrication costs and material waste.

In this thesis, the solution-processable method combined with synthesis and fabrication is explored as a two-step method.

1.5 Literature Survey

1.5.1 Transparent and Enzymeless Glucose Sensors

Transparent biosensors have been fabricated by various metal nanowire networks and other template-based metal networks and non-conventional lithographic techniques.[Bell et al., 2017] Crackle lithography has emerged as an unconventional method for fabricating a transparent metal mesh network.[Gupta et al., 2014, 2017b] Using this technique, a transparent Au metal wire network is prepared as a current collecting electrode and functionalized with redox-active species to fabricate a transparent glucose sensor. In an enzymeless glucose sensor, electrocatalysts play an important role in ascertaining its efficiency and performance.[Claussen et al., 2012] Various nanomaterials of noble metals,[Tian et al., 2014] metal oxides,[Zhu et al., 2016] nitrides,[Xie et al., 2018b, 2018a] carbides[Wu et al., 2017b] and chalcogenides[Zhu et al., 2018] with different morphologies, shape, size, and crystallinity have been employed as an active electrocatalytic material for fabrication of glucose sensors. Ni-based nanomaterials are well known as efficient electrocatalysts due to their easily reversible redox couple.[Chen et al., 2016; Karikalan et al., 2016; Mao et al., 2018] Moreover, Ni is also abundant and cost-effective, making it highly suitable for glucose sensing. The nanostructured Ni/NiO and their composite materials with a high surface area are usually synthesized by various techniques such as electrodeposition, physical vapor deposition, anodization, and hydrothermal synthesis. Literature is bound with enormous glucose sensors based on nickel oxide nanostructures due to

their high sensitivity, specificity, and selectivity.[Niu et al., 2013] Various three-dimensional, porous architectures with a high surface area are fabricated to improve the sensor characteristics such as operating voltage, detection range, sensitivity, and limit of detection (LOD). Shen *et al.* used a one-step method for fabrication of glassy carbon electrode modified with Ni nanoparticles-Attapulgite-GO hybrid electrode using an electrodeposition technique that showed LOD as low as 0.37 µM.[Shen et al., 2016] The cobalt nitride nanowire array on Ti mesh using a hydrothermal method was synthesized for glucose and hydrogen peroxide sensing in alkaline solutions. The high sensitivity of 3325.6 $\mu A.mM^{-1}\ cm^{-2}$ and LOD limit of 50 nM was achieved; however, the large-scale synthesis of the material is difficult because of the multiple steps and time involved in the fabrication of electrodes (Figure 1.5a).[Xie et al., 2018a] The hierarchical $Ni(OH)_2$ hollow nanorods were synthesized using chemical bath sonication for obtaining high sensitivity of 2904 $\mu A.mM^{-1}\ cm^{-2}$ and LOD limit of 2 µM; however, the linear detection range is only up to 3.86 mM and does not meet the physiological range of glucose levels (Figure 1.5b).[Yang et al., 2016] The Ni-doped diamond-like carbon film was synthesized using a magnetron radio frequency co-sputtering process. The fabricated electrodes showed a high sensitivity up to 10 mM glucose concentration without any influence of interfering species with excellent reversibility for glucose detection (Figure 1.5c). [Liu et al., 2018a] The electrodes were fabricated by electrodeposition to form coral-like Cu nano-structure arrays. The fabricated glucose sensor exhibited a limit of detection as low as 0.04 µM (Figure 1.5d).[Liu et al., 2018d]

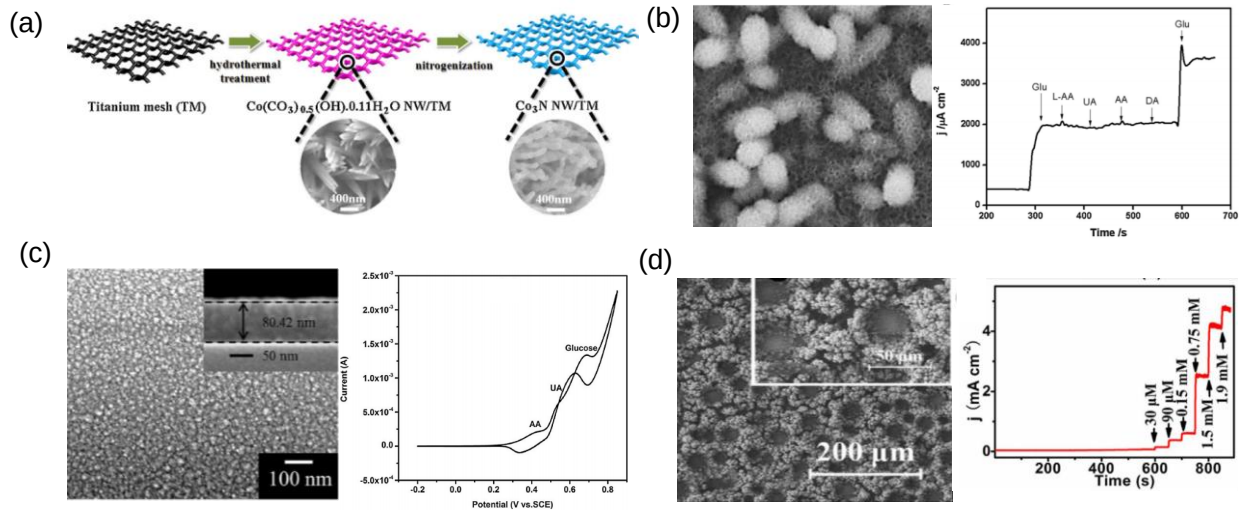

Figure 1.5: Literature reports of various techniques (a) hydrothermal (b) chemical bath sonication (c) radiofrequency sputtering (d) electrodeposition used in the fabrication of electrodes for glucose sensing. Figures are adapted from reference [Xie et al., 2018a], [Yang et al., 2016], [Liu et al., 2018a], and [Liu et al., 2018d], respectively.

Table 1.1: A brief literature survey of Glucose Sensors fabricated using Ni-based functional electrodes.

S.No	Electrode material	Voltage (V)	Sensitivity µA/(mM cm^2)	LOD (µM)	Reference
1	Ni-C-B Doped Diamond Hybrid Electrode	0.5	1374.4	1	[Gao et al., 2016a]
2	Ni-Co-CNTs	0.45	695	1.2	[Ramachandran et al., 2016]
3	Ni_7S_6	0.45	37.77	0.15	[Carbon et al., 2018]
4	Ni/B-diamond electrode	0.46	N.A	0.05	[Dai et al., 2016]
5	Ni-MOF/Ni/NiO/C GCE	0.65	367450	0.8	[Dai et al., 2018b]
6	Ni/graphene	0.50	388.4	0.79	[Ji et al., 2017b]

7	Ni/GO	0.50	535.25	2.8	[Ji et al., 2017a]
8	Ni-Co/Fe_2O_3	0.43	2171	0.19	[Vennila et al., 2017]
9	$NiCo_2O_4$/Au	0.45	0.3871	1	[Li et al., 2018]
10	Pd-Au-Ni / GCE	N.A	0.1322	1.7	[Lu et al., 2018]
11	Ni Crosslinked $Ni(OH)_2$ nanosheets	0.46	2761.6	0.46	[Mao et al., 2018]
12	NiS/C	0.47	1223	0.02	[Kubendhiran et al., 2018]
13	Ni_3N/GCE	0.55	39	0.48	[Luo et al., 2018a]
14	NiO petals	0.5	3.9	1	[Shu et al., 2018b]
15	Ni-Co-P	0.55	303	0.4	[Shu et al., 2018a]
16	$Ni_3(PO_4)_2 \cdot 8H_2O$/NF	0.45	2439	24.39	[Padmanathan et al., 2018]
17	Ni_3N-Co_3N	0.55	4418.7	0.03	[Dai et al., 2018a]
18	Metallic Nitride	0.55	7688	0.06	[Xie et al., 2018b]
19	Au-$NiCo_2O_4$	0.4	44.86	5	[Naik et al., 2018]
20	G-ZnO /Ni foam	0.8	1635.52	50	[Miao et al., 2018]
21	NiO /Ni foam	0.47	2739.5	0.75	[Zhang et al., 2018d]
22	Ni(OH)/CNTs	0.46	1220	0.645	[Qian et al., 2018]
23	$Ni(OH)_2$/RGO/Cu_2O/Cu foil	0.65	5350	0.35	[Wu et al., 2018]
24	NiO/Fe_2O_3	0.46	1437	1.03	[Jana et al., 2018]
25	$NiCo_2O_4$	0.5	4120	0.5	[Luo et al., 2018b]
26	NiO /ZnO	N.A	13.14	1	[Jung et al., 2018]
27	Ni@Pt/RGO	0.6	N.A	8	[Ma et al., 2018]
28	NiCo layered double hydroxide/G	0.6	344	0.6	[Asadian et al., 2018]
29	RGO-$NiCo_2O_4$ nanorods	0.55	960.37	0.35	[Ni et al., 2018]
30	Ag/Ni-Co layered double hydroxide	0.4	71.42	0.66	[Xu et al., 2018]
31	$Ni(SC_4H_9)_2$/Au film	0.6	171.12	0.737	This work
	$Ni(SC_4H_9)_2$/Au film		564.7	11.827	
	$Ni(SC_4H_9)_2$/Au mesh		675.97	2.167	
	$Ni(SC_4H_9)_2$/Au mesh		325.74	7.170	
	$Ni(SC_4H_9)_2$/FTO		852.05	6.082	

1.5.2 Ni and Co oxides for OER

The catalyst of noble metals such as Pt, Ir, and Ru work efficiently for oxygen evolution reactions (OER).[Reier et al., 2012] Earth-abundant 3d-transition metal oxides (Figure 1.6a), [Kim et al., 2018b; Xu et al., 2020a] sulfides,[Dai et al., 2017; Su et al., 2017] (Figure 1.6b) and phosphides (Figure 1.6c) [Qiu et al., 2019] [Jin, 2017] of cobalt have been proven as promising candidates for their efficient performance that can be achieved via precise control over composition and structure.[Anantharaj et al., 2016; Hisatomi et al., 2014; Kim et al., 2016; McCrory et al., 2015] Xu et al. have used simple NiO obtained from Ni-MOF for fabrication of electrode where the overpotential value was as low as 410 mV. Dai et al. has used Cobalt monophosphosulfide and achieved a lower potential as low as 266 mV. Qiu and coworkers have worked on cobalt phosphide to obtain an overpotential of 300 mV. Wang et al. have studied in-situ spectroscopy of cobalt oxide, and an onset potential of 220 mV was obtained. Various materials have been explored in literature reports for the fabrication of OER-based

electrodes. Co oxide-based materials have attracted increasing attention with the merits of the extensive source, low price, and expected endurance in the working environments.[Deng et al., 2017a; Limburg et al., 2012] These display highly active surface sites with moderate conductivities, making them good candidates for electrocatalysts. In addition, the spinel-type structure with different oxidation states and coordination environments (i.e., octahedral and tetrahedral sites) results in completely tunable water splitting behavior.[Bergmann et al., 2015; Deng et al., 2014; Koza et al., 2012] In Co_3O_4, spinel structure is known to convert to layered oxy-hydroxide by increasing the valance state with the application of the positive potential, thus offering much higher surface sites for OER (Figure 1.6d).[Wang et al., 2016a]

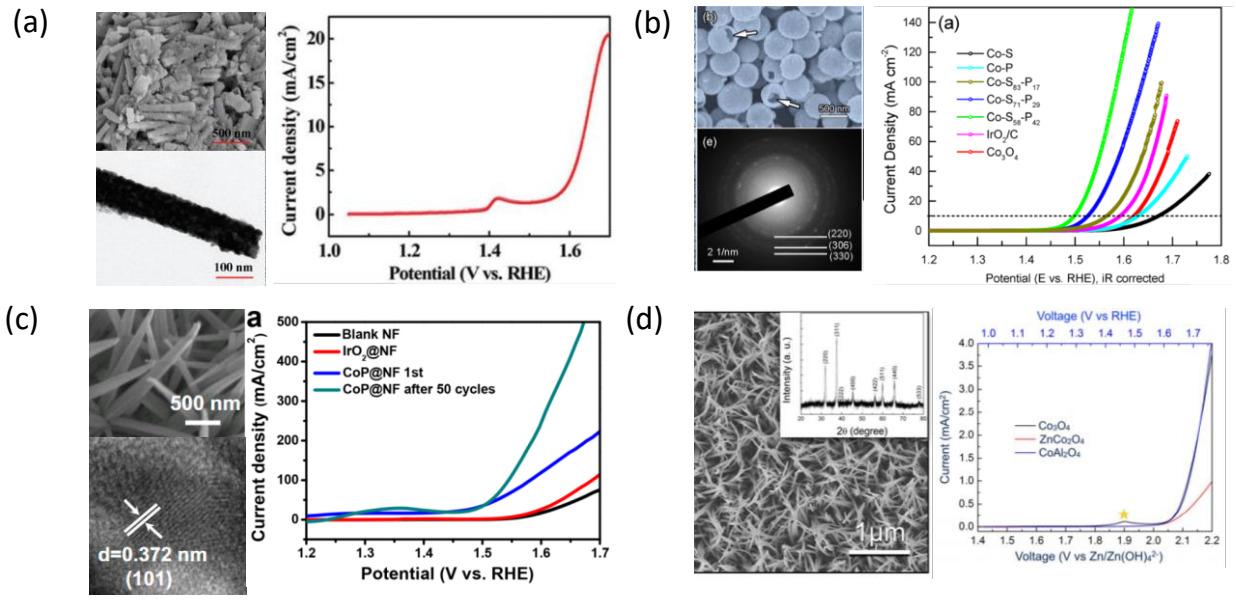

Figure 1.6: Various materials explored for OER in literature reports (a) Nickel oxide, (b) Cobalt monophosphosulfide, (c) Cobalt phosphide, and (d) Cobalt oxide. Figures are adapted from reference [Xu et al., 2020a], [Dai et al., 2017], [Qiu et al., 2019], and [Wang et al., 2016a], respectively.

Electrocatalytic activity, such as overpotential and stability, still needs improvement to reach the performance of the rare-earth metal electrocatalysts. There are various factors that affect electro-catalytic water splitting such as particle size,[Barakat, N., Khil, M., Sheikh, 2008] catalyst loading,[Liang et al., 2011] crystallinity,[Vineesh et al., 2016], pH of the electrolyte,[Yang et al., 2018a] operating temperature,[Zhang et al., 2018a] surface morphology and preparative material conditions.[Zhu et al., 2017b] Moreover, the loading density and accessibility of active sites of the catalyst by electrolyte are important for the superior performance of the catalyst. With these considerations,[Lyu et al., 2017, 2019a, 2019b] current fabrication methods such as hydrothermal and microwave synthesis,[Chen et al., 2015] sol-gel,[Mattos-Costa et al., 1998] and spray pyrolysis[Li et al., 2005] adopted for the synthesis Co_3O_4 nanostructures are increasingly becoming complex and non-scalable.

Table 1.2: Literature comparison among cobalt-based OER systems

S. No	Catalyst	Electrolyte	Overpotential @10 *mA*/cm² (mV)	Tafel Slope (mV/dec)	Reference
1	Co embedded N-doped graphene	1 M KOH	430	—	[Hou et al., 2015]
2	Cobalt phosphide N-doped C nanostructures	1 M KOH	320	49	[Zhu et al., 2017a]

3	ZIF-67-derived Co-NC@CoP-NC Nanostructure	0.1 M KOH	330	79	[Li et al., 2016]
4	In situ CoO-Co/N-doped C	1 M KOH	290	82	[Jin et al., 2015]
5	CO_3O_4 nano crystals on reduced GO	0.1 M KOH	310	67	[Liang et al., 2011]
6	N-doped grapheme supported Co@CoO nanoparticles	1 M KOH	350	68	[Zhang et al., 2016a]
7	Co embedded N doped carbon nanotubes	0.1 M KOH	200	50	[Wang et al., 2015]
8	$Co_3(PO_4)_2$ nanoparticles embedded in doped C	1 M KOH	290	82	[Feng et al., 2018]
9	Co Nanoparticles embedded in N doped C	1 M KOH	371	61	[Su et al., 2014]
10	Co_3O_4@CS	1 M KOH	290	61	[Singh et al., 2018]
11	Co_3O_4@CC	1 M KOH	300	77.06	This work

1.5.3 $NiCo_2O_4$ Nanoplates for OER

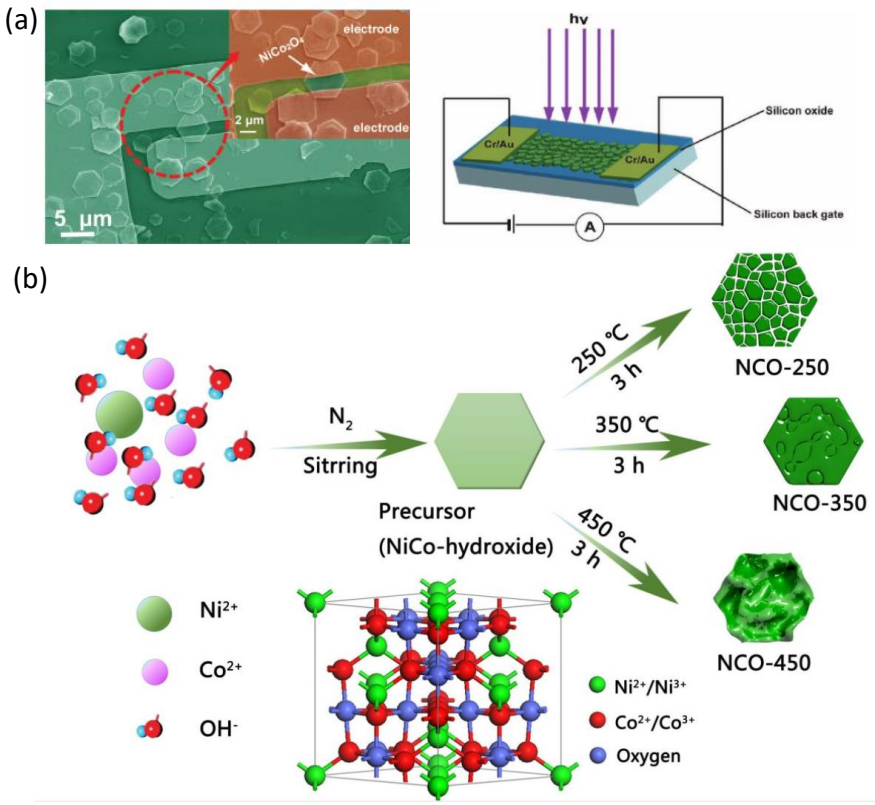

Figure 1.7: Nickel cobaltite nanoplates synthesized using hydrothermal methods for application in (a) photoelectric and catalytic applications and (b) OER. Figures are adapted from reference [Liu et al., 2015] and [Zhao et al., 2018]

The world energy crisis has led to the trend to solve the problems in energy production, conversion, and storage. Exhaustive research has been carried out on energy conversion and storage using solar cells, photocatalysis, electrocatalysis supercapacitors, lithium-ion batteries,

and metal-air batteries to meet crisis challenges. Electrode material plays an essential role in real-time application because performance depends upon various physical and chemical parameters. Various materials have been studied in the literature on electrocatalysis and water splitting. Noble metals and metal oxides have been widely explored. Among all these materials, $NiCo_2O_4$ is of particular interest as it is one of the promising electrode materials for various applications. For example, compared with pristine NiO and Co_3O_4, the $NiCo_2O_4$ has 2 orders of higher electrical conductivity. The high electronic conductivity in nickel cobaltite favors the faster transfer of electrons, facilitating its application as electrode material. It is not only the electronic conductivity, but the simultaneous contributions from Co^{3+}, Co^{2+}, Ni^{3+}, Ni^{2+} redox couples from both Ni and Co offer richer redox chemistry, resulting in a higher catalytic and electrocatalytic activity. Nickel cobaltite has been explored in the areas of photoelectric and catalytic applications (Figure 1.7). Hydrothermal method, co-precipitation method, microwave-assisted method, sol-gel method, electrodeposition method, and dry synthesis are the most commonly used methods for the synthesis of nickel cobaltite. Considerable efforts have been made in the literature to synthesize nickel cobaltite by morphologies and structures such as nanorods, nanoneedles, nanoplates, nanowires, etc., for enhanced electrocatalytic applications. In this thesis work, we have mainly used nickel cobaltite for application in OER. Various composites, e.g., nitrogen-doped graphene with nickel cobaltite, were synthesized using a hydrothermal method, which gave an overpotential of 373 mV. [Chen et al., 2013a] Nickel cobaltite nanosheets were synthesized for application in OER, resulting in the overpotential value of 270 mV. [Fang et al., 2018] Fe-doped nickel cobaltite was used as an OER electrode (336 mV). [Deng et al., 2017b] However, the nickel cobaltite-based electrode materials explored from solution-processable methods are rare cases.

Table 1.3: Literature comparison among Ni-Co oxide catalyst-based OER systems.

S.No	Material	Overpotential @ 10 mA/cm^2	Tafel slope (mV/dec)	TOF (s^{-1})	Electrolyte (M)	References
1	N-Graphene @$NiCo_2O_4$	373 at 5 mA/cm^2	156	N.A	0.1 M KOH	[Chen et al., 2013a]
2	$NiCo_2O_4$	290	53	N.A	1 M NaOH	[Gao et al., 2016b]
3	$NiCo_2O_4$/Ni_2P Nanocones	250	58	N.A	1 M KOH	[Wang et al., 2017]
4	$NiCo_2O_4$ nanosheets	270	59.2	N.A	1 M KOH	[Fang et al., 2018]
5	P-$NiCo_2O_4$ Nanowire	300	120	N.A	1 M KOH	[Chu et al., 2020]
6	Co_3O_4/$NiCo_2O_4$/ Ni Foam	320	84	2.87@ 320 mV	0.1 M KOH	[Yang et al., 2019]
7	$NiCo_2O_4$-MCNTs hybrid	350	67	0.032 @ 370 mV	0.1 M KOH	[Umeshbabu et al., 2020]
8	$NiCo_2O_4$@Ni_xCo_y\LDH/NF	193	37.59	N.A	1 M KOH	[Li et al., 2019a]
9	$NiCo_2O_4$	346	72	N.A	1 M KOH	[Shrine Maria Nithya Jeghan and Gibaek Lee, 2017]
10	$NiCo_2O_4$	265	82	N.A	1 M KOH	[Chen et al., 2018]

11	$Ni_xCo_{3-x}O_4$ Nanowire	N.A	59	N.A	1 M NaOH	[Li et al., 2010]
12	CFP/$NiCo_2O_4$/C $o_{0.57}Ni_{0.43}$LMOs	340	63	0.0446 @340 mV	0.1 M KOH	[Yin et al., 2016]
13	$Ni_xCo_{3-x}O_{4-y}$ 3D nanocages	320	53	N.A	1 M KOH	[Antony et al., 2016]
14	Fe-$NiCo_2O_4$	336	36	0.033 @ 350 mV	1 M KOH	[Deng et al., 2017b]
15	$MnCo_2O_4$	327	79	N.A	1 M KOH	[Lankauf et al., 2020]
16	P123-$NiCo_2O_4$	350	109	N.A	1 M NaOH	[Devaguptapu et al., 2017]
17	NCO-20/CC	310	68.5	0.039 @ 350 mV	1 M KOH	This work

1.5.4 $NiCo_2O_4$ Nanoplates for Biomolecular Sensing

Researchers have explored various materials for simultaneous detection that include various metal-oxides carbon-based materials, etc. MnO_2 nanowires embedded with electro-reduced graphene oxide electrodes were synthesized for dopamine detection. [He et al., 2019] TiO_2 reduced graphene oxide composite electrodes were fabricated for highly efficient detection of ascorbic acid [Harraz et al., 2019]. The graphene ZnO composite was obtained using one-pot synthesis for simultaneous detection of ascorbic acid, dopamine, and uric acid.[Zhang et al., 2016b] High-performance one-dimensional MgO nanostructures were synthesized for simultaneous detection of biomolecules (Figure 1.8a-d).[Li et al., 2014] In this context, spinels are one of the best choices, easily used for electrochemical detection because of the rich redox chemistry compared to metal oxide.[Chang et al., 2015; Luo et al., 2019; Shi et al., 2014; Zhao et al., 2017] Nickel cobaltite as a spinel is one such material that has drawn the attention of many researchers in the fields of catalysis, supercapacitor, rechargeable metal-air batteries, and water splitting owing to its phenomenal properties.[Gao et al., 2016b; Huang et al., 2017; Liu et al., 2015; Trivedi et al., 2017; Wang et al., 2016b; Yang et al., 2017]

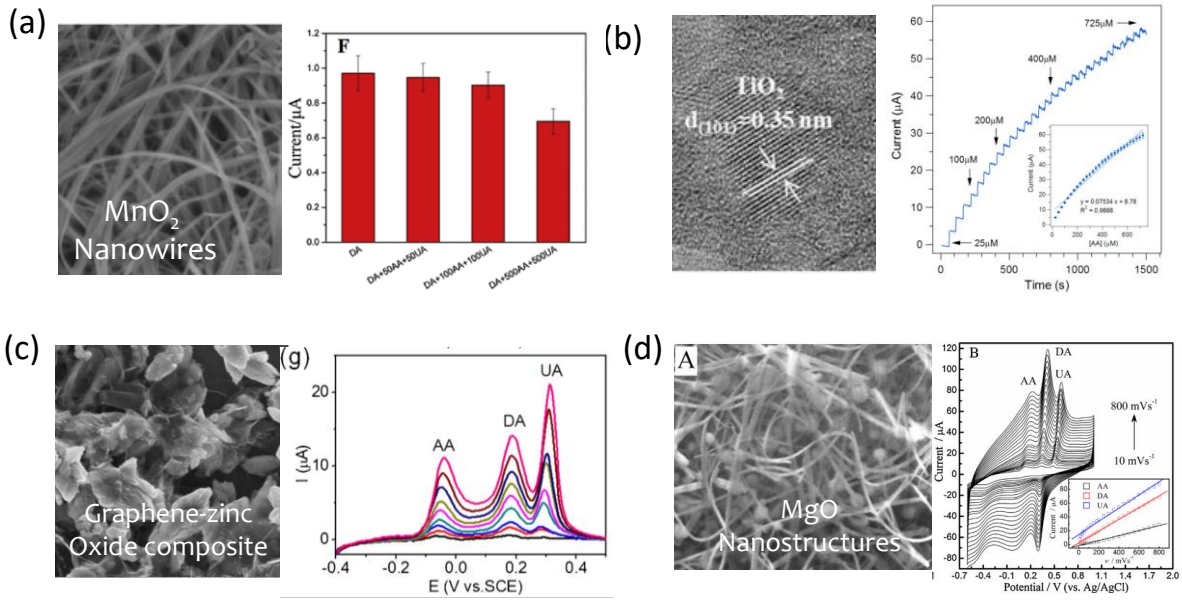

Figure 1.8: Materials like (a) MnO2 Nanowires (b) TiO2 graphene Composite (c) Graphene-Zinc oxide composite, and (d) MgO Nanostructures with their corresponding electrochemical responses. Figures adapted from references [He et al., 2019], [Harraz et al., 2019], [Zhang et al., 2016b], and [Li et al., 2014] respectively.

Table 1.4: Comparison of electrochemical sensors for simultaneous determination of AA, DA, and UA.

S.No	Material /Substrate	Analytes	LOD	Detection Range	Reference
1	GCE/Au-polydopamine nanospheres	AA DA UA TR	0.2 nM 0.1 nM 0.1 nM 0.1 nM	10–80 µM and 80–240 µM; 1–160 µM and 160–350 µM; 10–120 µM and 120–350 µM; 1–160 µM and 160–280 µM	[Arroquia et al., 2020]
2	rGO/Pd@PPy –GCE	AA DA UA	0.049 µM 0.056 µM 0.047 µM	0.04-12000 µM 38-1647 µM 1.4-219 µM	[Demirkan et al., 2020]
3	GOx/Pt NPs/PANI/MEA	Glucose UA Cholesterol	260 µM 4 µM 440 µM	2–12 mM 0.1–1.2 mM 1–12 mM	[Gao et al., 2019]
4	GQDs-MWCNTs/GCE	DA	0.87 nM	0.005 -100 µM	[Huang et al., 2020]
5	GQDs/IL-SPCE	AA DA UA	6.64 µM 0.06 µM 0.03 µM	25–400 µM 0.2–10 µM 0.5–20 µM	[Kunpatee et al., 2020]
6	MIP-MWCNTs/GCE	DA Epinephrine	0.015 µM 0.023 µM	0.04 -70 µM 0.04 -70 µM	[Liu et al., 2020]
7	Cu2O/Cu@C core-shell NWs	UA	0.4 µM	0.05 to 1.1 mM	[Luo et al., 2020]
8	Nitrogen-doped graphene/PDDA/gold nanoparticle	UA	53 nM	0.5-100 µM	[Pang et al., 2020]
9	Nano-Cu-PSAIII/GCE	AA DA UA	0.15 µM 0.01 µM 0.10 µM	0.30-730 µM 0.02-65 µM 0.25-107 µM	[Zhang et al., 2013]
10	Hierarchical nanoporous Pt-Ti alloy	AA DA UA	24.2 µM 3.2 µM 5.3 µM	0.2 - 1 µM 0.004 - 0.5 µM 0.1 - 1 µM	[Zhao et al., 2016]
11	Pristine graphene	AA DA UA	6.45 µM 6.45 µM 4.82 µM	9.00 -2314 µM 5.00 -71 µM 6.00 -1330 µM	[Qi et al., 2015]
12	Graphene ink	AA DA UA	17.8 µM 1.44 µM 0.29 µM	50 -1000 µM 3 - 140 µM 0.5 - 150 µM	[Fu et al., 2018]
13	Zn-NiAl LDH/rGO superlattice	AA DA UA	13.5 µM 0.1 µM 0.9 µM	0.5 – 11 µM 0.001 – 1 µM 0.001 – 0.9 µM	[Asif et al., 2019]
14	Fe_3O_4-SnO_2-Gr	AA DA UA	62.0 µM 7.1 µM 5.0 µM	0.1 -23 µM 0.02 - 2.8 µM 0.015 - 2.40 µM	[Bagheri et al., 2017]
15	PPy hydrogel/GCE	AA DA UA	1.28 µM 0.04 µM 0.04 µM	2.5 –1500 µM 0.08–250 µM 0.25–400 µM	[Wang et al., 2019a]

16	rGO incorporated L-lysine	AA DA UA	2000 µM 100 µM 150 µM	100 –1200 µM 2 – 60 µM 20 -200 µM	[Zhang et al., 2017]
17	ZnNi@f-MWCNT	AA DA UA	0.51 µM 0.065 µM 0.0882 µM	200 -1200 µM 250 -1700 µM 200 -900 µM	[Savk et al., 2019]
18	N_2/Ar/GS/GNR	AA DA UA	0.0053 µM 0.0025 µM 0.0057 µM	0.1 –1400 µM 0.01 –400 µM 0.02–350 µM	[Jothi et al., 2018]
19	Herringbone CNTs	AA UA	15 µM 15 µM	15-600 µM 15-420 µM	[Abellán-Llobregat et al., 2018]
20	$NiCo_2O_4$/CC	DA UA	0.7 nM 0.6 nM	0.001-1000 µM 0.001-1000 µM	This work

1.5.5 Conversion of Polystyrene to Graphitic Carbon

The estimated production of expanded polystyrene is around 3 million tons annually in the world. After use, polystyrene is typically land-filled, which takes not only a significant space but also a huge time to degrade.[Fonseca et al., 2015; Li et al., 2012] The recycling rate of polystyrene is very less due to the high cost of collection and storage compared to the low value of recycled polystyrene.[Gong et al., 2013] Therefore, recycling is not a viable option, but polystyrene can be converted into high-value, conducting carbon material for multiple applications, which is more feasible, attractive, and commercially sustainable. Carbon materials are the best choice as an electrode materials due to their high conductivity, surface area, and chemical stability.[Bahuguna et al., 2018, 2019] Carbon obtained from polystyrene has been utilized as electrode material for application in energy storage devices, surface adsorption for removal of pollutants from water, and other catalytic applications.[Gupta et al., 2012; Wen et al., 2015; Zhang et al., 2019a, 2018c]

The disordered carbon from waste polystyrene has been used for application in sodium-ion batteries (Figure 1.9a).[Fonseca et al., 2015] The hierarchical porous carbon using cross-linked polystyrene, melamine, and iron chloride was used for the oxygen reduction reaction (Figure 1.9b).[You et al., 2014] The high surface area porous carbon was synthesized using polystyrene for methane gas storage (Figure 1.9c).[Gatti et al., 2019] The carbonized polystyrene-based reticulated resin for dibenzothiophene adsorption.[Wang et al., 2009] However, polystyrene is practically difficult to carbonize because, on heating, it degrades from larger molecules to form a complex mixture of low-molecular-weight volatile compounds with polycyclic aromatic hydrocarbons (PAHs) at the intermediate temperature range of 450 °C, which is much below the temperature (600 °C) required for carbonization of any polymer.[Ogenko et al., 2007] In literature, as an alternative to direct carbonization of polystyrene, polystyrene-based macro reticular resins have been prepared and carbonized.[Du et al., 2019a; Wang et al., 2019b; Wen et al., 2019a] Paula *et al.* pyrolyzed polystyrene dissolved in acetone in a vertical furnace at 530 °C in an argon atmosphere for 5 h to obtain the carbon material with further KOH activation at 800 °C to increase the surface area[de Paula et al., 2018] Zhang *et al.* synthesized 3D structured porous carbon through Fridel-Crafts reaction using cross-linked polystyrene as carbon source and silica particles for templating (Figure 1.9d).[Zhang et al., 2018b] Min *et al.* used autoclaved polystyrene with MgO flakes as a hard template to obtain a flake-like structure at 700 °C for 2 h.[Min et al., 2019b]

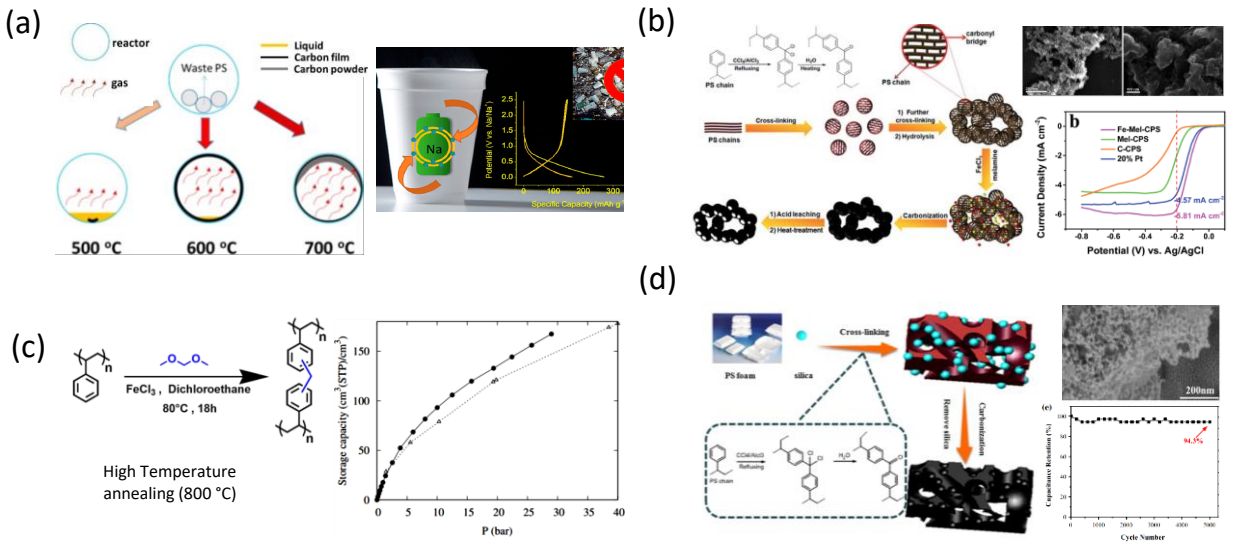

Figure 1.9: Different methods used for the synthesis of graphitic carbon (a) sealed high-pressure reactor, (b) Non-templated pyrolysis (c) Friedel-craft reaction with high temp annealing (d) Silica templated carbonization. Figures are adapted from reference [Fonseca et al., 2015], [You et al., 2014], [Gatti et al., 2019] and [Zhang et al., 2018b]

Table 1.5: Literature survey of carbon-based EDLCs derived from waste polymers.

S. No.	Material and Precursor	C_{sp} (3-electrode) F/g @ A/g	C_{sp}(2-electrode) F/g @ A/g	Electrolyte	Cycles A/g	C retention %	Reference
1	Onion Peel to hierarchical porous carbon	127 @ 0.75	98 @ 0.1	1 M H_2SO_4	2000 @ 0.75	109	[Mehare et al., 2020]
2	Polystyrene to 3d network of porous carbon	208 @ 1	162 @ 0.5	6 M KOH	5000 @ 5	94.3	[Zhang et al., 2018c]
3	Mixed Plastic waste to porous carbon nanosheets	207 @ 0.2	N/A	6 M KOH	N/A	N/A	[Wen et al., 2019a]
4	Polystyrene to ordered mesoporous carbon	118 @ 0.2	N/A	6 M KOH	5000 @ 2	87.2	[Liang et al., 2019]
5	Polystyrene to porous carbon flakes	119 @ 1	50 @ 1	6 M KOH	1000 @ 10	93.4	[Min et al., 2019b]
6	Polystyrene to 3D hierarchically porous carbon	284.1 @ 0.5	69.3 @ 0.5	6 M KOH	10000 @ 10	90.2	[Ma et al., 2020]
7	Polystyrene foam to multichannel	271.6 @ 0.5	212.5 @ 0.5	1 M H_2SO_4	5000 @ 0.5	100	[Ishita et al., 2020]

	carbon nanofibers						
8	Polystyrene/polyacrylonitrile to carbon spheres	451.5 @ 0.5	406 @ 0.5	6 M KOH	10000 @ 2	75.5	[Du et al., 2019b]
9	Polystyrene foam	327 @ 1	N/A	1 M H_2SO_4	10000 @ 1	100	[Deka et al., 2020]
10	poly(ethylene terephthalate) to carbon nanosheets	169 @ 0.2	N/A	6 M KOH	5000 @ 10	90.6	[Wen et al., 2020]
11	Willow wood to activated carbon	395 @ 1	201 @ 0.5	6 M KOH	5000 @ 5	94	[Phiri et al., 2019]
12	Rice Straw to nitrogen-doped porous carbon	317 @ 1	269 @1	6 M KOH	5000 @ 10	99.4	[Xu et al., 2020b]
13	Polyethylene to Hollow mesoporous carbon cages	200 @ 1	150 @ 1	6 M KOH	5000 @ 5	94.6	[Zhang et al., 2019b]
14	Sugar-Polymer composite to graphitic carbon	158 @ 1	39 @ 1	3 M KOH	10000 @ 4	90	This work

Although carbonization of various waste plastics has been explored, the carbonization of waste polystyrene and the applications of the polystyrene-derived carbon for energy storage devices is relatively less studied. It is due to the presence of mesoporous insulating templates such as silica, alumina, sand, MgO, etc., that affects the overall resistance of the carbon powder.[Cabo et al., 2010; Gupta et al., 2012; Kyotani et al., 1995; Min et al., 2019a; Wen et al., 2019b] The processing steps involved in template removal and KOH activation deteriorate the conductivity and crystallinity of carbon despite its high specific surface area. Specifically, in electric double-layer capacitors (EDLCs), crucial factors that determine the electrochemical performance and efficiency are the accessibility of the ions to the electrode surface, conductivity, pore size distribution, wettability, thermal stability, and chemical stability of the electrode material. [Deka et al., 2020; Du et al., 2019b; Palaniselvam et al., 2015; Yuan et al., 2016] Even though the high surface area and porous structures facilitate the increased accessibility of electrolyte ions; however, the quality in terms of graphitic content and crystallinity is equally important for reducing the internal resistance of the electrode. The graphitic carbon with an optimum surface area and conductivity usually result in excellent capacitive performance with high energy and power density and long duration of life cycles.[Xiong et al., 2015, 2017] Because of all these associated challenges, polystyrene-derived carbon has been seldomly reported in the literature for high-performance EDLC supercapacitors.

1.6 Scope of the Thesis Work

The main objective of this thesis is to focus on the scalable aspect of nanomaterials using solution-processable inks on flexible and 3D substrates without the need for binders. The idea is to fabricate electrodes without the particular need for multi-step methods and sophisticated

techniques for electrochemical biosensing and energy applications. However, certain limiting factors are addressed in this thesis to overcome adhesion issues, ease of fabrication, stability, scalability, and applicability. The aim is to fabricate electrodes with high performance, stability, and activity with economic viability for large-scale applications in energy and sensing.

The scope of each research chapter (3-7) of the thesis work is as follows:

1. Glucose sensors have been extensively explored in literature. However, the fabrication of a non-enzymatic sensor with a lower and wider range of detection with a simple process and low cost is a challenging task. In this work, the Ni-BT complex was electro-oxidized on Au network electrodes for the fabrication of glucose sensors. The higher sensitivity of the Ni-BT/Au mesh electrodes is due to the effective diffusion of ionic species and better current collection resulting in a lower detection range.
2. Co hexadecanethiolate (Co-HDT) and Ni butane thiolate (Ni-BT) Inks were used as precursors for the formation of Co_3O_4 and NiO electrocatalysts supported on the 3D substrates. A layer-by-layer (LbL) dip-coating method is developed for the high loading of ink for the best performance in OER. The method developed in this study is advantageous as it does not require any conductive binders and can be extended over a large scale. The work is focused on studying the electrochemical behavior of electrodes fabricated by the LbL method towards enhancing the performance of OER and comparing it with the conventional dip-coating method. The material and processing adopted in this work play an important role in achieving highly efficient energy materials.
3. Nanostructured nickel cobaltite spinels are an important choice of electrocatalyst due to their high electronic conductivity, activity, and stability. In this work, we have reported a scalable and solution-processable method for the fabrication of Ni-Co spinel nanoplates on carbon cloth by thermolysis of Ni-Co thiolate hybrid inks. As per our knowledge, it is the first report involving the formation of superparamagnetic, ultrathin, bimetallic spinel nanoplates using the supramolecular organization of mixed metallomesogens. Under optimized synthetic conditions of concentration, the composition of precursors, temperature of annealing, and gas environment, Ni-Co hybrid ink yielded 2D nanoplates, which exhibit excellent OER performance in terms of low overpotential and Tafel slope and long term stability. The high catalytic performance is found to be related to the unique nano-morphology, surface composition, and crystallinity of $NiCo_2O_4$ nanoplates. An increment in magneto-current density is obtained under a moderate magnetic field due to the superparamagnetic nature of the thin nanoplates. The $NiCo_2O_4$ spinel on carbon cloth proves to be an effective and efficient OER electrocatalyst system in comparison to that of other similar reports in the literature.
4. Simultaneous electrochemical detection of dopamine and uric acid are important biomarkers in the physiological examination, is challenging because of the narrow range of oxidation peak potentials. The nickel cobaltite nanoplates synthesized in the above work were further used as a sensing platform for the simultaneous detection of dopamine and uric acid. The performance of $NiCo_2O_4$ was found to be superior to Co_3O_4 and NiO due to multiple oxidation states and higher conductivity. Nickel cobaltite, due to the high catalytic activity, shows higher sensitivity and better response for simultaneous detection with excellent specificity and anti-interference properties.
5. In another study, a novel method for the conversion of polystyrene to graphitic carbon is developed. In the literature, complex processes involving large amounts of expensive catalysts, high temperature, and pressure conditions are used for the conversion of polymers to graphitic carbon that is not easily adaptable on a commercial scale. Secondly, the structural and electrical properties of graphitic material are largely compromised. However, in this work, a unique approach is developed using waste polystyrene as a raw carbon source, sugar as a soft template, and solution-processed Ni-

butanethiolate as a catalyst for the synthesis of graphitic carbon. The graphitic carbon with microporous nature and high crystallinity are obtained by this method that is ideally suited for high-performance EDLC supercapacitors.

To achieve the objectives laid out in the study, various characterization techniques, measurements, and analysis methods have been carefully used throughout the work. The experimental conditions are rigorously optimized for reproducible data collection, and error analysis is done over several measurements while reporting the results presented in the thesis work.

1.7 Conclusion

This chapter presents an overview of the synthesis, properties, and applications of Ni-Co nanostructured electrodes fabricated using Ni-Co-based alkanethiolates as functional inks. A detailed literature survey of the materials, fabrication, and synthesis techniques has been carried out. Various basic principles of operation, synthesis of the active materials, electrode fabrication, and various applications have been discussed. The above chapter clearly lays the scope and the objectives of this thesis work carried out. Several potential applications of Ni-Co-based oxides, such as biosensors, water splitting (OER), and supercapacitors, are elaborated in detail in this introductory chapter of the thesis.